Observations from Tests on a Segmental Bridge

RICHARD M. McCLURE, HARRY H. WEST, and P.C. HOFFMAN

ABSTRACT

The Pennsylvania Department of Transportation designed and constructed a posttensioned segmental concrete box-girder bridge at the Pennsylvania Transportation Research Facility (Test Track) located at Pennsylvania State University. The bridge consists of two independent curved girders with a simply supported span length of 121 ft (36.9 m). The cross section of each girder consists of a box section with side cantilevers. The main objectives of the research program for the segmental bridge were to make field measurements on the full-scale bridge, to study the behavior of the bridge under normal truck loadings, and to study the overload behavior to establish actual safety factors. The accomplishment of these objectives required temperature studies, static load testing of the bridge, overload testing of the bridge, laboratory testing of individual segments, and theoretical studies. This research resulted in many observations for the design of segmental bridges concerning temperature, longitudinal bending, and transverse bending.

The United States is faced with the severe problem of bridge deterioration. It has been reported that 105,000 of the 564,000 bridges in the United States are in critical need of repair or replacement (1). There is no simple answer to solving the problem of replacing and repairing these deteriorated bridges. The task of correcting the structures will undoubtedly require many different technologies and methods.

One of the answers to this problem is the use of precast, prestressed-concrete segmental construction in which the benefits of both precasting and posttensioning can be combined advantageously. This combined method has been shown to be an efficient and economical method of construction (2).

Segmental bridge construction originated in the United States about three decades ago. In 1952 the Freyssinet Company designed a segmental I-girder bridge in New York State; however, the technique of segmental construction was not commercially applied on a large scale until 1962, when the Choisy-le-Roi Bridge was built over the Seine River in Paris (2). Since then segmental construction has spread throughout Europe, and the technique has been continuously refined (3). Segmental construction is now gaining worldwide acceptance, with much use in the United States.

Engineers concerned with the problems of bridge repair or replacement are constantly looking for innovations and improvements in bridge quality and economy. To this end, an experimental segmental bridge was designed and constructed by the Pennsylvania Department of Transportation (4).

A letter survey was also conducted as part of the project. The purpose of the letter survey was to gather information on current designs and construction problems as well as to assess the state of the art concerning segmental concrete box-girder bridges in the United States. The results of this survey pointed out the need for the establishment of national design and construction criteria (5). Since this survey, two reports on the subject have been published by the Prestressed Concrete Institute (PCI) (6,7).

The main objectives of the research program for the experimental segmental bridge were to make field measurements on the full-scale bridge, to study the behavior of the bridge under normal truck loadings, and to study the overload behavior to establish actual safety factors. The accomplishment of these objectives required temperature studies, static load testing of the bridge, overload testing of the bridge, laboratory testing of individual segments, as well as theoretical studies.

TEST BRIDGE

The experimental segmental bridge was constructed at the Pennsylvania Transportation Research Facility (Test Track), which is located at Pennsylvania State University. This facility is an oval-shaped highway, 1 mile in length, which was built primarily for pavement and bridge research.

The configuration of the bridge had to match the existing alignment of the facility, and the span length was controlled by the existing abutments. Because of the curvature at the bridge locations, the curved girders have full superelevation and are on a grade. The general plan, elevation, and cross section of the experimental bridge are shown in Figure 1. The bridge consists of two identical

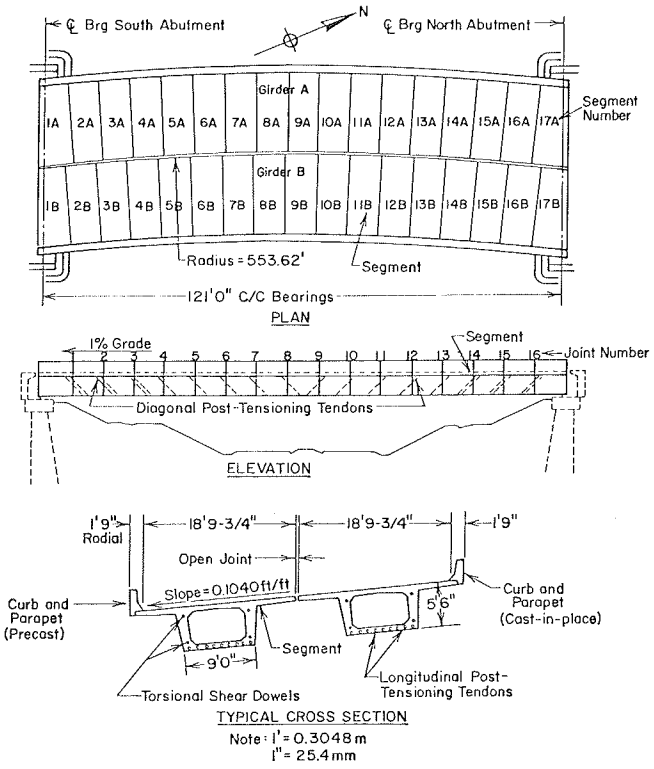

FIGURE 1 General plan, elevation, and typical section.

simply supported girders with segments and joints numbered as shown. It should be noted, however, that most segmental bridges have continuous spans. Each independent girder consists of 17 segments that are tied together with longitudinal bar or strand posttensioning tendons plus diagonal bar posttensioning tendons. Steel shear dowels were used to achieve alignment during construction and to transfer torsional moment after the girders were built. Epoxy was used as the main jointing material between the segments. An open longitudinal joint between the girders was selected to allow an independent comparison of the two girders.

The design specifications for the experimental bridge were from the Standard Specifications for Highway Bridges of AASHTO (8). These were supplemented by the Pennsylvania Department of Transportation's Design Manual (9).

The curved box girder was designed for longitudinal moment by using straight beam theory for the dead load, AASHTO HS20-44 live loading, and prestress. The design was made by using allowable stresses and was checked for ultimate strength. For transverse moment, the segments were designed elastically as a box frame with side cantilever flanges. At the bottom of the webs the frame was assumed to be simply supported.

Each girder was analyzed for torsion as a horizontally curved beam with eccentric loads. Torsional design was based on a method presented by Zia and McGee (10). The cross section of the segments was approximated as a box section with the flanges neglected.

The ability of the joints to provide friction was considered only for ultimate strength conditions. Accommodations for flexural shear were provided by the posttensioned diagonal bar tendons, and the steel shear dowels were designed to resist torsional shear between segments. These joint details are not necessarily representative of current practice.

End diaphragms were introduced in the end segments, which were ample in size to take the substantial reaction forces from the neoprene bearings pads and torsional anchorages and to provide room for the posttensioning end anchorage plates. In addition, an opening was made to allow easy access by researchers to the inside of the box section.

The segments for the experimental bridge were cast individually at a fabrication plant by the short-line method in one steel form with provisions for adjustments. They were then hauled about 100 miles (161 km) to the facility, where they were erected on steel scaffolding-type falsework.

TEMPERATURE STUDY

The main purposes of this study were to determine the dimensional level that needs to be considered in the heat flow problem for a bridge structure; to observe the temperature distributions that occur within a cross section over a 1-year period, as well as to identify the meteorological conditions associated with extreme temperature distributions; and to measure bridge movements under the different observed temperature distributions.

Instrumentation

The instrumentation for measuring temperatures consisted of an Estherline Angus-Model E 1124 E multipoint recorder and 24 copper versus constantan thermocouples that were located at various positions on the cross section (11,12). The thermocouple placement was performed after bridge erection by drilling and filling the void with an epoxy that was specified by the manufacturer as thermally compatible with the concrete (11).

The average vertical deflections at midspan were measured by using six dial gauges, with two placed at each end and two placed at midspan. The dial gauges were mounted to produce vertical deflections that were perpendicular to the bottom of the girder (11).

Longitudinal Variation

The initial portion of the thermal study considered the possibility of a longitudinal temperature variation. This investigation compared 10 thermocouple readings at hourly intervals for 3 different daily cycles between segments 2A and 5A, and segments 2A and 9A (see Figure 1).

The collected ordered pairs of readings for like thermocouple positions were then analyzed by simple linear regression. From the regression analysis it was concluded that there was no significant longitudinal temperature variation (11). The longitudinal study reduced the heat-flow problem from a three-dimensional analysis to one with no more complexity than two dimensions.

Transverse Variation

The second portion of the study observed the transverse temperature distributions of the bridge for 18 daily cycles during the period starting on October 25, 1978, and ending on October 16, 1979. The set of 18 daily observations was designed to indicate seasonal extremes as best as could be predicted by the researchers before the measurements. Each transverse temperature distributon was compiled hourly from the 24 thermocouple readings (11).

It was found that there was little transverse temperature variation in the horizontal direction. Therefore, the heat-flow problem could be further reduced from a two-dimensional to a one-dimensional state with the vertical temperature variations resulting in vertical deflections only (11).

Vertical Deflection and Vertical Temperature Distribution

The effect of the seasonal variation on vertical deflection has been reported previously (11,12). The observations indicated that the maximum upward deflection was 0.72 in. (18.29 mm); it occurred on July 7, 1979. Also, the maximum downward deflection was 0.11 in. (2.79 mm); it occurred on January 4, 1979. The thermal conditions on the two dates were completely opposite (11).

The thermocouple readings on July 7, 1979, that corresponded to the maximum upward deflection of 0.72 in. indicated a maximum surface temperature differential of 51°F (28.3°C) between the top and midheight to the girder.

Specifications

Currently, U.S. design codes do not specify the consideration of a vertical temperature distribution. However, the New Zealand specification requires the consideration of a fifth-power temperature distribution for webs and cantilever flanges, as shown in Figure 2a. Also, the deck slab above the cells and the soffit are subjected to a linear temperature distribution, as shown in Figure 2a. The PCI and the Post-Tensioning Institute (PTI) recommended as simplier vertical thermal distribution, as shown in Figure 2b, where the flange is uniformly warmer than the remaining cross section (12).

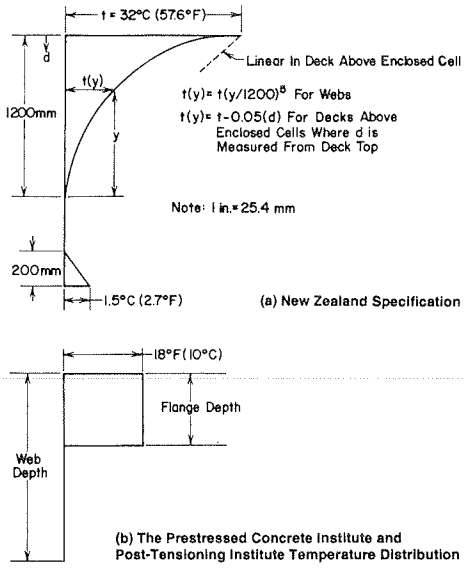

FIGURE 2 Thermal distribution assumptions for design.

Comparisons

A comparison of the temperature distributions with the New Zealand specification indicates satisfactory agreement. The observed maximum surface temperature differential of 51°F is reasonably close to the New Zealand recommendation of 57.6°F (32°C). Also, the field observations for the webs indicate that the critical temperature distribution that causes maximum upward bowing can be approximated by a fifth-order polynomial. In addition, the slab above the box cell showed a linear temperature distribution (11).

The observed curvature, which was calculated from measured vertical deflections, was compared with theoretical curvatures, which were calculated from both the modified New Zealand specification and the modified PCI-PTI temperature distribution. In the modified New Zealand specification the vertical temperature distribution varied as a fifth-order polynomial from 51°F at the top surface to 0°F (-17.8°C) at a depth of 47.24 in. (1200 mm). In the modified PCI-PTI method the temperature was assumed to be 35.8°F (19.9°C) in the 8-in. (203-mm) flange, which is approximately twice the recommended value, and 0°F elsewhere. The observed curvature for a 0.72-in. (18.3-mm) midspan deflection agreed closely with curvatures calculated from the modified New Zealand and PCI-PTI distributions (12). However, residual temperature stresses calculated from the two vertical temperature distributions differed markedly (12).

STATIC LOAD TESTING

The main purpose of the static load testing of the full-scale experimental bridge was to study the elastic longitudinal bending behavior of girder A under actual live-load conditions. The tests focused mainly on the determination of experimental deflections and strains from which stresses were determined. The test results were compared with results from a finite-element analysis and from a conventional analysis. Numerous comparisons were made between observed and calculated quantities, but only two are reported here. More comparisons are available in a report by McClure and West (13).

Testing and Instrumentation

The test vehicle for these tests was loaded to conform as closely as possible to AASHTO HS20-44 live loading plus additional loading to account for the effects of impact (8). The loading arrangement for the vehicle is shown in Figure 3. The test vehicle traveled from north to south and occupied three lateral positions on girder A during the static load tests. First, the center of the vehicle was 5 ft (1.52 m) to the left of the girder centerline while the vehicle crossed. On the next two passes the center of the vehicle was centered and 4 ft (1.22 m) to the right of girder centerline, respectively (13).

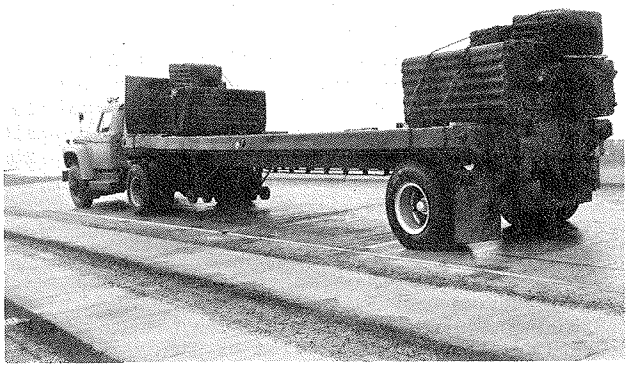

FIGURE 3 Test vehicle for static load tests.

During the tests measurements were made to determine live-load deflections by using dial gauges, and live-load strains were determined by using electrical resistance strain gauges. The readings for the deflections when using dial gauges were taken manually, which required the test vehicle to be stopped when the front axle was at odd-numbered joints so that the readings could be taken. The readings for strains were recorded continuously by using a Honeywell Accudata System with a half-bridge hookup for temperature compensation as the test vehicle traveled at approximately 1.0 mph (1.6 km/h). Therefore, two separate runs were needed to obtain a complete set of readings (13).

The live-load deflections for various positions of the test vehicle were measured by using six dial gauges that were located on the bottom of girder A. At each end, two dial gauges were located at the lower corners of the box approximately 1.5 in. (38 mm) from the abutment pedestal. Two dial gauges were similarly located at midspan. The desired deflection was taken as the average value at the center of the span with respect to the average values at the end gauge locations. All measurements were perpendicular to the bottom of the girder, which resulted in deflections that were also perpendicular to the bottom (13).

Measurements to determine live-load strain for all positions of the test vehicle were made by using electrical resistance strain gauges located at the middle of segment 9A, which is at midspan. This segment was chosen because of the high live-load bending moment at that location (13). The locations of the metal foil electrical resistance strain gauges are shown in Figure 4.

Deflections

Both experimental and theoretical values of vertical deflection are plotted in Figure 5 according to the

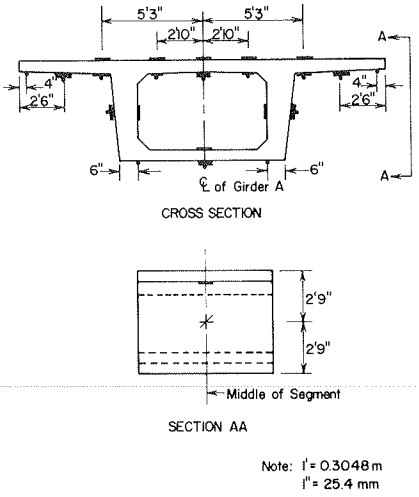

FIGURE 4 Locations of electrical resistance strain gauges on segment 9A for static load tests.

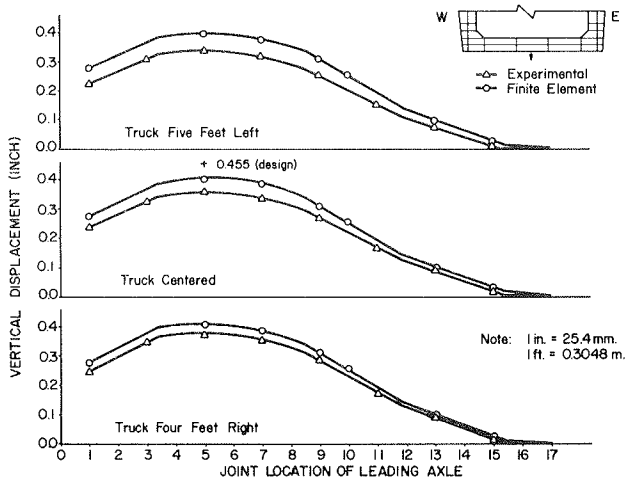

FIGURE 5 Midspan centerline vertical deflections for static load tests.

position of the leading axle of the truck loading. The main theoretical values were determined by using an elastic finite-element analysis for prestressed-concrete structures with the use of SAP IV. The structural analysis program (SAP) is a general purpose finite-element program that was developed at the University of California at Berkeley. The SAP IV version, first released in June 1973 and revised in April 1974, was used in this study (14).

The variation in midspan deflection as a function of load position is theoretically composed of straight-line segments when all three axles are either to the left or the right of midspan. Discontinuities occur in the straight-line segments when an axle enters or leaves the span. However, the variation is curved in those regions where there are axle loads on both sides of midspan (13). The curves shown in Figure 5 are drawn through the data points to reflect these conditions.

An examination of the data in Figure 5 indicates that the experimental results are consistently lower in value than the finite-element results, with a maximum discrepancy of about 15 percent. This tendency for the actual bridge to be stiffer than the finite-element model was reflected throughout the study (13).

Also displayed in Figure 5, for the truck-centered case, is the midspan deflection associated with the leading axle at joint 5 based on the conventional beam theory approach. This deflection of 0.455 in. (11.56 mm) is about 14 percent greater than the corresponding finite-element value, which indicates that the conventional approach used in the design employs a model that is even less stiff than the finite-element model (13).

Longitudinal Stresses

If the bridge is treated approximately as a straight member, and if it is assumed to be loaded and to respond in the vertical plane, then the maximum midspan moment will vary piecewise linearly as the truck moves across the span. Discontinuities occur as an axle enters the span, crosses over midspan, or leaves the span (13). A standard influence line approach gives a maximum midspan moment of 2,228 ft-kips (3021 kN•m) when the leading truck axle is at joint 7. This moment reduces slightly to 2,133 ft-kips (2892 kN•m) when the leading axle is at joint 5. Because longitudinal flexural stress is a direct function of bending moment, this stress will have the same piecewise-linear variation as does the moment when the truck passes over the bridge (13).

The longitudinal stresses on the bottom centerline surface of the box section for segment 9A are compared in Figure 6. The variation patterns in stress as the truck passes over the span show excellent correlation between the experimental and finite-element results. Also, the trend observed earlier in the displacement comparisons is substained here; that is, the experimental results are approximately 15 percent less than the finite-element results (13).

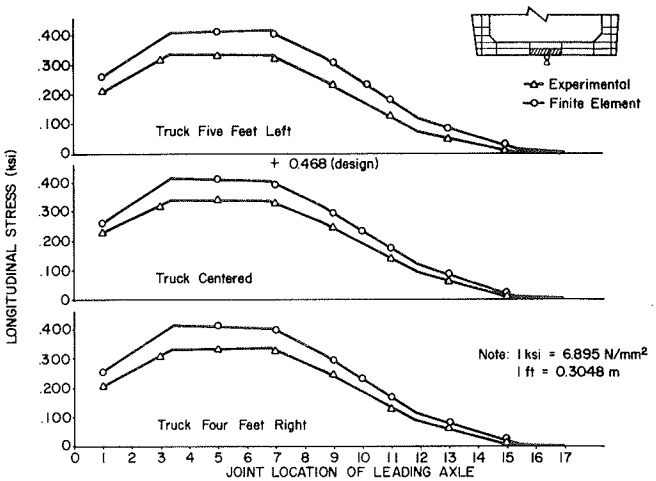

FIGURE 6 Bottom flange longitudinal stresses for middle of segment 9A for static load tests.

Based on standard flexural stress calculations, and by using the maximum midspan moment of 2,228 ft-kips for the simplified straight beam and the section modulus from the design computations, the maximum flexural stress is 0.468 ksi (3.23 N/mm²) (13). This stress is shown in Figure 6 for the truck-centered case with the leading axle at joint 7, and it is seen to be larger than both the finite-element and experimental values.

OVERLOAD TESTING

The main purpose of the overload testing was to study the inelastic longitudinal bending behavior of girder B under overload conditions. The tests focused mainly on the determination of experimental deflections and strains from which stresses were determined. The test results were compared with the results from a finite-element analysis and from a conventional analysis. Numerous comparisons were made between observed and calculated quantities, but only a few will be reported here. More comparisons are available in a report by McClure et al. (15).

Testing and Instrumentation

Girder B was tested with static loading by using the loading frames shown in Figure 7. The loading frames include four hydraulic tension jacks. Four openings

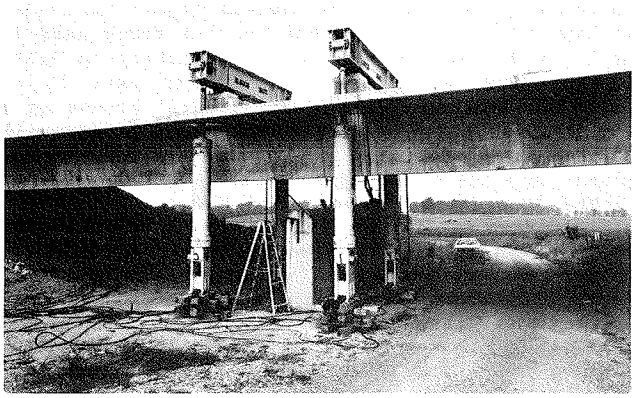

FIGURE 7 Loading frame for overload tests.

for the jacks were cut through the concrete bridge deck directly above the jacks. The jacks were hinge-connected to the steel loading beams at their top ends and attached to the anchor assembly of the rock anchors at their lower ends. The rock anchors were drilled and grouted approximately 75 ft (23 m) below the ground level, 20 ft (6 m) of which were in sound bedrock. Each rock anchor was capable of developing a load of 500 kips (2225 kN), which was equal to the capacity of the loading beams used for the testing. Each loading beam consisted of two 27 x 114 wide flange beams placed on a roller support at one end and a hinged support at the other. The beams delivered the loads through 2-in.-thick (50.8-mm) steel plates to concrete pedestals located over the webs to give a longitudinal bending type failure. The load schedule called for an initial load of 186 kips (887.4 kN), with daily increments of 100 kips (444.8 kN) until failure occurred. The loads were monitored by separate pressure gauges for each jack and verified from strain readings on each ram (15).

Deflections for all load increments were measured by using dial gauges. Three gauge lines located at the bottom of the girder were used as was previously described for the static load tests. All dial gauges determined the displacements in a direction perpendicular to the bottom surface of the girder. After the girder started yielding, the deflections were measured with an engineer's level, which was set up at a distance from the girder, and two level rods, which were permanently mounted at the midspan of the girder (15).

Strains at the middle of segment 9B were measured at each load increment by using metal foil electrical resistance strain gauges. This segment, which is at midspan, was chosen because of the large bending moment at that location. These longitudinal strain gauges were placed as shown in Figure 8. Only longitudinal gauges were used because bending was of primary interest. All strains were read with a Model P-350 Budd Strain Indicator, which used a half-bridge circuit with temperature compensation gauges (15).

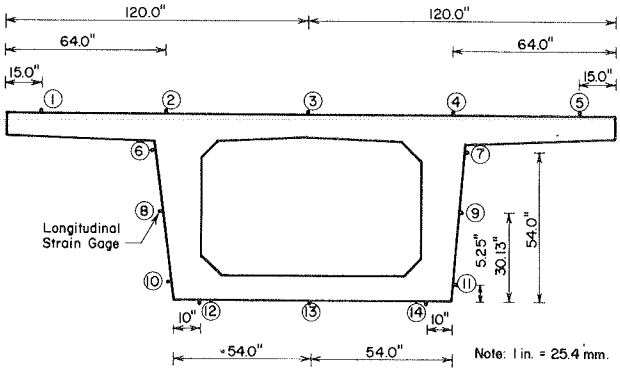

FIGURE 8 Location of electrical resistance strain gauges on segment 9B for overload tests.

Deflections

To obtain the total experimental deflection at midspan for any load, the permanent set was added to the measured deflection. This was necessary so that all experimental deflections were measured from the same origin. The experimental and theoretical midspan deflections are shown in Figure 9. The data in

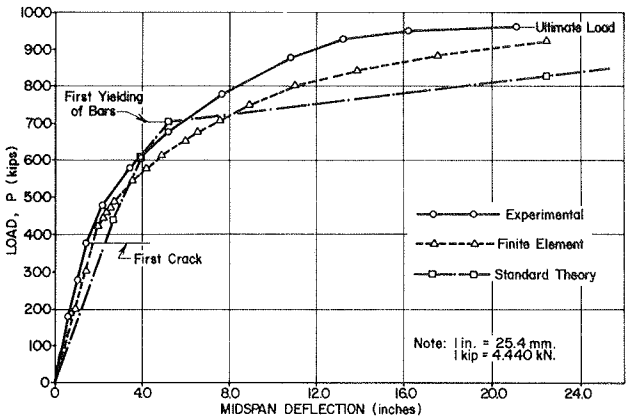

FIGURE 9 Load deflection diagrams for girder B for overload tests.

the figure indicate satisfactory agreement between finite-element and observed deflections at all load levels, with the finite-element model once again indicating less stiffness than the real structure. The finite-element analysis was once again performed by using SAP IV, which was extended beyond yielding by using the inelastic properties of the materials (15). Figure 9 also shows the results of a conventional prestressed-concrete beam analysis by using strain compatibility (16), which indicates satisfactory agreement with experimental values up to first yielding.

Longitudinal Stress

The permanent set strains should be added to the measured strains to obtain the absolute surface strains that should be with the theoretical strains. However, permanent set strains were not measured. Comparison of measured and finite-element strains did indicate fair agreement up to first yielding, where permanent set strains were small but did reveal a deviation of results above first yielding where the permanent set strains were relatively large (15). Figure 10 shows the comparison of observed and finite-element strains at the middle of segment 9B for a load of 376 kips (1672 kN), which is below first yielding.

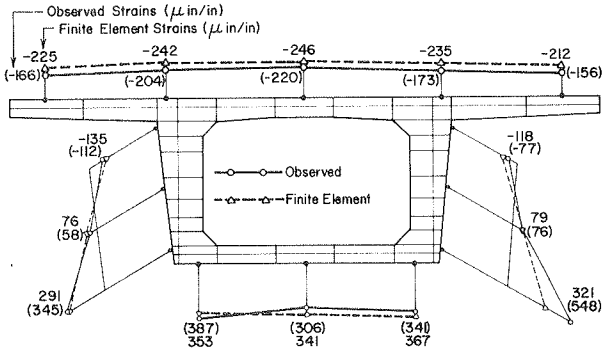

FIGURE 10 Longitudinal surface strains at middle of segment 9B for a load of 376 kips (1672 kN) for overload tests.

Cracking and Failure

In the first and second days of testing, up to load P = 276 kips (1228 kN), there was no visible cracking on the bottom surface of the bridge. In the third day of testing, at load P = 376 kips (1672 kN), the first visible cracking was observed at the bottom surface between the points of loading. As the load was increased, cracks increased in number, and those between the points of loading widened and extended toward the compression zone. Nothing unusual was noticed until the eighth day of testing at a load of 876 kips (3896 kN), when two loud sounds were heard at different times and the pressure gauge readings for the jacks dropped down slightly. It sounded like a strand or bar tendon had broken each time. At this load the cracks at joints 8 and 9 opened widely and extended upward toward the top slab.

In the last day of testing, at load P = 945 kips (4203 kN), two events occurred: first, a noise was heard and the deflection increased suddenly by 0.25 in. (6.35 mm); second, two strong sounds, similar to those that occurred at P = 876 kips were heard, and again, deflection increased suddenly by another 0.25 in. Pressure readings started to fall off, but then reached a constant value. As the load was slightly increased to a load of 955 kips (4248 kN), the crack at joint 8 opened widely and the concrete in the compression zone crushed and spalled on the surface. The mode of failure of the bridge is shown in Figure 11. On inspection of joint 8, it was found that all the longitudinal strands were broken and only the bar tendons were holding the bridge in place.

The finite-element load at first cracking was estimated at P = 420 kips (1868 kN), which is 12 percent larger than the observed value. The cracking load calculated from conventional theory was P = 439 kips (1953 kN), which is 5 percent larger than the corresponding finite-element value. Also, the finite-element load at failure was estimated at P = 920 kips (4092 kN), which is 4 percent smaller than the observed value. The failure load calculated from conventional theory by using strain compatibility was P = 901 kips (4000 kN), which is 2 percent smaller than the corresponding finite-element value (15).

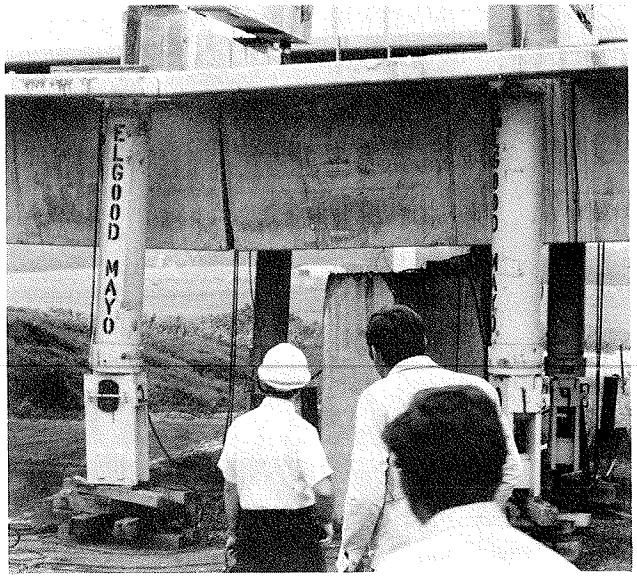

FIGURE 11 Mode of failure of girder B.

LABORATORY TESTING

The main purpose of the testing of individual segments was to establish transverse bending behavior to augment the data obtained from field testing the experimental bridge. The individual segments were tested under simulated field conditions to determine failure modes. Experimental results were compared with the results from a conventional approach that used a frame analysis in the elastic range and yield-line theory to predict ultimate behavior of the slab. Numerous comparisons were made between observed and calculated quantities, but only a few will be reported here. More comparisons are available in a report by McClure et al. (17).

Testing and Instrumentation

Four individual segments were tested under simulated field conditions in the structures laboratory at Pennsylvania State University. Each concrete segment was supported between two steel end frames approximately the shape of the segment, as shown in Figure 12. The end frames had provisions for torsional shear dowels, diagonal tendons, and longitudinal posttensioning bars that could be tensioned to induce the desired longitudinal stress conditions. The four segments were tested statically for several loading positions. In the tests the loads were positioned along the middle of the segment to simulate wheel loads from a standard truck.

Measurements were taken with dial gauges to determine transverse deflections at the middle of the segment. Measurements were also taken with wire electrical resistance strain gauges to determine strains at the middle of the segment. All strains were read with a Model P-350 Budd Strain Indicator, which used a half-bridge circuit with temperature compensation gauges (17).

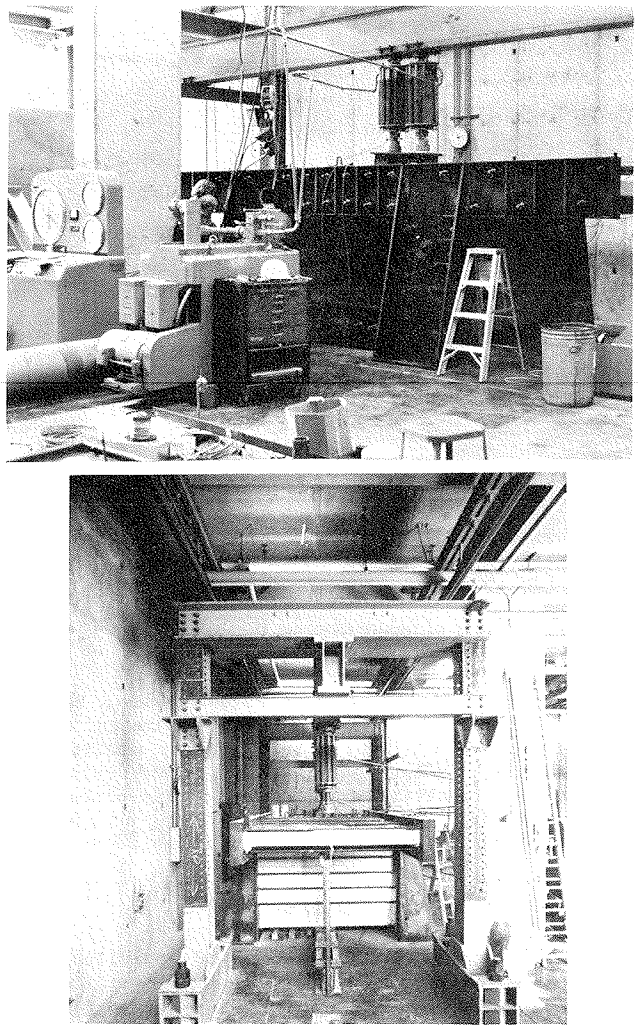

FIGURE 12 Test setup for testing of segments: front view (top), and side view (bottom).

Deflections

The results of the tests indicated that the only significant deflections were the vertical deflections of the top slab that were maximum at the ends of the cantilevers. Deflections at other locations were extremely small. Deflections at the end of the flange are shown in Figure 13. The data in this figure indicate that the amount of longitudinal posttensioning stress in the slab also affects the flange deflection.

The theoretical flange deflection curves shown in Figure 13 are for a simple cantilever without friction along the edge of the flange. The theoretical curve used elastic theory up to first cracking and was modified for inelastic stresses above first cracking.

Moments

Experimental and theoretical transverse moments were compared to determine the reliability of the frame design process in the transverse direction. All of the experimental and theoretical moments were for the middle of the segment, where the moments are a maximum because the loads are applied at the middle of the segment. The moments are for two static loads of 20 kips (89 kN), which represent the standard AASHTO wheel loads plus an allowance for impact.

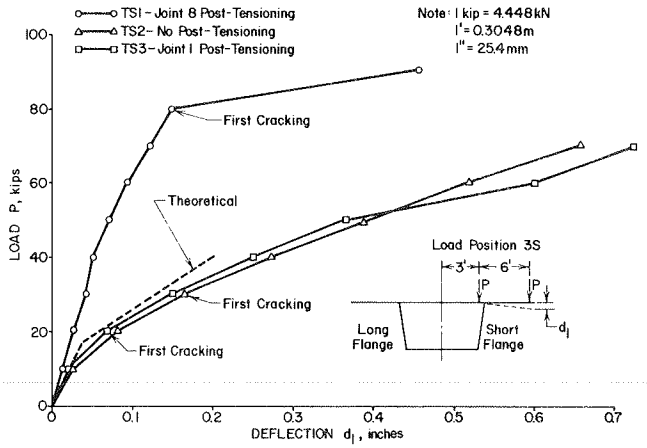

FIGURE 13 Deflection of flange in transverse direction at middle of segment.

Strains from the electrical resistance strain gauges were used to establish the experimental strain distribution at any section. The stresses and forces at that section could then be determined, and the experimental transverse moments were calculated by using statics. The theoretical transverse moments were calculated by the method used for the design of the segments. This procedure is based on the moment distribution method of analysis for a rigid frame, and the load is assumed to be distributed over a length of segment (17).

A comparison of experimental and theoretical moments indicated that transverse bending moments are the largest in the top slab, and that in almost all cases the experimental moments are smaller than the theoretical moments (17).

Cracking and Failure

All cracking and failures during the laboratory transverse bending tests occurred in the top slab of the segments. Theoretical cracking loads were calculated by neglecting the end frames and treating the sections as doubly reinforced slabs. The flanges were treated as cantilevers, and the top slab of the box section was treated as a part of a rigid frame. Theoretical ultimate loads were calculated by using yield-line theory for the top slabs. A simple support was assumed at the end frames, and a fixed support was assumed along the tops of the webs. Satisfactory agreement was observed between experimental and theoretical cracking and failure loads (17).

OBSERVATIONS

- Curvature because of temperature is constant along the length of girder. Therefore, the heat-flow problem can be reduced from a three-dimensional to a two-dimensional state.
- Little transverse temperature variation occurs in the horizontal direction. Therefore, the heat-flow problem can be further reduced from a two-dimensional to a one-dimensional state, with temperature variation occurring in the vertical direction only.
- For a statically determinate or indeterminate structure, residual stresses develop because of restrained strain from a nonlinear vertical temperature variation. These residual stresses can be calculated by direct analysis if the vertical variation in temperature is known.

- For a statically indeterminate structure, the curvature from vertical temperature variation is also important in the design. Either a fifth-order vertical temperature distribution across the entire cross section (New Zealand gradient) or a uniform vertical temperature distribution in the top slab (PCI-PTI gradient) can be used to predict the curvature.
- Reinforcing steel must be provided to carry the total tensile force if the temperature stresses caused by the nonlinear vertical temperature distribution or continuity-induced stresses exceed the ultimate tensile stress of the concrete.
- Elastic deflections and stresses from longitudinal bending can be adequately predicted by using the finite-element method, with the finite-element values about 15 percent larger than the actual values. A conventional design can also be used to conservatively predict the values, with the conventional values consistently larger than the finite-element values. Some economy in design might be achieved by using the finite-element method of analysis in the design.
- Inelastic deflections and stresses from longitudinal bending can be adequately predicted by using the finite-element method. The conventional design approach of using strain compatibility can be used to conservatively predict the failure load, but it should not be used to predict inelastic deflections.
- The only significant transverse deflections in a segment are in the top slab. These deflections occur under the wheel loads and are maximum at the end of the cantilever flanges. The elastic transverse deflections can be predicted by treating the cross section as a rigid frame.
- Transverse moments have a maximum value at a cross section under the wheel loads. Elastic transverse moments can be conservatively predicted by using a frame analysis, where the frame consists of a box section with side cantilevers.
- Transverse bending failures of the top slab were the primary mode of failure, with the flanges being the weakest part of the segment. Theoretical transverse cracking loads can be predicted by treating the cross section as a rigid frame. Theoretical transverse failure loads can be predicted by using yield-line theory for the slab, with a simple support assumed at the edge of segment and a fixed support assumed along the top of webs.

ACKNOWLEDGMENT

A portion of a major 6-year investigation on an experimental segmental bridge that was conducted at the Pennsylvania Transportation Institute, located at the Pennsylvania State University, was presented in this paper. The study was sponsored and funded by the Pennsylvania Department of Transportation and FHWA.

REFERENCES

1. One in Six U.S. Highway Bridges is Deficient. Engineering News Record, March 10, 1977, pp. 18-21.
2. J. Muller. Ten Years of Experience in Precast Segmental Construction. Prestressed Concrete Institute Journal, Vol. 20, No. 1, Jan.-Feb. 1975, pp. 28-61.
3. C.A. Ballinger, W. Podolny, Jr., and M.J. Abrahams. A Report on the Design and Construction of Segmental Prestressed Concrete Bridges in Western Europe--1977. FHWA, U.S. Department of Transportation, July 1978.
4. H.P. Koretzky and A.T. Tscherneff. Final Report--Research Project No. 72-9 on the Design of an Experimental Posttensioned Segmental Concrete Box Girder Bridge. Publication 118. Pennsylvania Department of Transportation, Harrisburg, Sept. 1974.
5. H.P. Koretzky and P.H. Kuo. Letter Survey on "State of the Art in the U.S.A. of Segmental Concrete Box Girder Bridges." Publication 114. Pennsylvania Department of Transportation, Harrisburg, July 1974.
6. Prestressed Concrete Institute, Joint PCI-PTI Committee on Segmental Construction. Recommended Practice for Precast Posttensioned Segmental Construction. Prestressed Concrete Institute Journal, Vol. 27, No. 1, Jan.-Feb. 1982, pp. 14-61.
7. Prestressed Concrete Institute, Bridge Committee. Tentative Design and Construction Specifications for Precast Segmental Box Girder Bridges. Prestressed Concrete Institute Journal, Vol. 20, No. 4, July-Aug. 1975, pp. 34-42.
8. Standard Specifications for Highway Bridges, 11th ed. AASHTO, Washington, D.C., 1973.
9. Design Manual. Publication 15. Pennsylvania Department of Transportation, Harrisburg, 1973, Part 4: Structures.
10. P. Zia and W.D. McGee. Torsion Design of Prestressed Concrete. Prestressed Concrete Institute Journal, Vol. 19, No. 2, March-April 1974, pp. 46-64.
11. P.C. Hoffman, R.M. McClure, and H.H. West. Temperature Studies for an Experimental Segmental Bridge. Interim Report. Pennsylvania Transportation Institute, Pennsylvania State University, University Park, June 1980.
12. P.C. Hoffman, R.M. McClure, and H.H. West. Temperature Study of an Experimental Segmental Concrete Bridge. Prestressed Concrete Institute Journal, Vol. 28, No. 2, March-April 1983, pp. 78-97.
13. R.M. McClure and H.H. West. Field Testing on an Experimental Segmental Bridge. Interim Report. Pennsylvania Transportation Institute, Pennsylvania State University, University Park, June 1980.
14. H.H. West and R.M. McClure. Full Scale Testing of a Prestressed Concrete Segmental Bridge. Proc., International Conference on Short- and Medium-Span Bridges, Toronto, Ontario, Canada, Aug. 1982.
15. R.M. McClure, H.H. West, and M. Abdel-Halim. Overload Testing of an Experimental Segmental Bridge. Interim Report. Pennsylvania Transportation Institute, Pennsylvania State University, University Park, July 1982.
16. A.H. Nilson. Design of Prestressed Concrete. Wiley, New York, 1978.
17. R.M. McClure, D.B. Anderson, and T.E. McDevitt. Laboratory Testing of Segments for an Experimental Bridge. Interim Report. Pennsylvania Transportation Institute, Pennsylvania State University, University Park, Feb. 1980.

Publication of this paper sponsored by Committee on Concrete Bridges.